Wang *et al. Chin. J. Mech. Eng.* (2018) 31:18
https://doi.org/10.1186/s10033-018-0209-6

Chinese Journal of Mechanical Engineering

ORIGINAL ARTICLE

Open Access

Sealing Performance and Optimization of a Subsea Pipeline Mechanical Connector

Li-Quan Wang[1], Zong-Liang Wei[1*], Shao-Ming Yao[2], Yu Guan[1] and Shao-Kai Li[1]

Abstract

Researchers seldom study the optimum design of a mechanical connector for subsea oil-gas pipeline based upon the sealing performance. An optimal design method of a novel subsea pipeline mechanical connector is presented. By analyzing the static metal sealing mechanism, the critical condition of the sealing performance is established for this connector and the formulation method of the contact pressure on the sealing surface is created. By the method the minimum mean contact pressure of the 8.625 inch connector is calculated as 361 MPa, which is the constraint condition in the optimum design of connector. The finite element model is created in ANSYS Parametric Design Language (APDL) and the structure is optimized by the zero-order method, with variance of contact pressure as the objective function, and mean contact pressures and plastic strains as constraint variables. The optimization shows that variances of contact pressure on two sealing surfaces decrease by 72.41% and 89.33%, respectively, and mean contact pressures increase by 31.18% and 52.84%, respectively. The comparison of the optimal connectors and non-optimal connectors in the water pressure experiments and bending experiments shows that the sealing ability of optimized connectors is much higher than the rated pressure of 4.5 MPa, and the optimal connectors don't leak under the bending moment of 52.2 kN·m. This research provides the formulation to solve contact pressure on the sealing surface and a structure optimization method to design the connectors with various dimensions.

Keywords: Mechanical connector, Sealing mechanism, Sealing performance, Critical condition, Minimum mean contact pressure, Variance

1 Introduction

The depletion of onshore oil-gas resource makes more attention paid to offshore oil-gas exploitation, particularly to the development of subsea resources [1]. In recent years, more and more devices, such as pipelines, riser systems, subsea trees, manifolds, tie-in systems, have been applied to the seabed [2]. Pipelines on the seabed tend to be damaged by unexpected artificial and natural interferences caused by fishing nets, anchors, wave oscillations, and other seabed features and seism [3]. Once pipelines are damaged, a series of problems will be produced, which has negative effects on society, economy, and environment [4]. Therefore, how to connect pipelines reliably as well as related equipment in setting up a subsea oil-gas production system and pipeline repair is a big challenge. Because of the restricted operating environment in the deep sea, non-weld connection is the best choice to connect the subsea pipeline.

Most of the non-weld connectors are supplied by offshore oil-gas service companies from America and Europe, such as Oil states industries Inc, Cameron, FMC Technologies, Oceaneering International Inc, Quality Connector LLC and Hydratight. Static metal seal based Connectors include tapping connector and method of using same [5], swivel ring flange, external hydraulic tieback connector [6], subsea tool for tie in of pipeline ends [7] and adapter sleeve for wellhead housing [8]. Rubber sealed connectors include pipeline joint [9], over 2000 morgrip connector and coupling device [10]. The other connectors with metal and rubber seal include griplock end connector, smart flange plus connector, quick flange morgrip pipeline connector and hydraulic smart flange connector. The above typical connectors are reliable to

*Correspondence: weizongliang1207@163.com
[1] College of Mechanical and Electrical Engineering, Harbin Engineering University, Harbin 150001, China
Full list of author information is available at the end of the article

connect subsea pipelines, but their design is too complicated. Too many bolts have to be pre-tightened and operation tools have to be used for connection, which result in a long lead time and high cost. Gottfried [11] presented a simple metal sealing connector for the connection of water supply and drainage pipelines with diameter less than 168.3 mm under low or zero pressure on land. This paper presents an improved design of subsea pipeline mechanical connector (SPMC) that can be used for a bigger diameter and a higher pressure in the complicated subsea environment.

Taking the advantages of low and high temperatures, low and high pressures and corrosion, the metal sealing gaskets are suitable for oil-gas exploitation, chemical industry and nuclear industry, where rubber seals are prohibited [12]. SPMC is a static metal seal without gasket, and the optimal sealing performance is the key technology. Up to now the researches of the pipeline connection are extensive, but few of them focus on the design of connector without gasket. In the design of a connector with gasket, the gasket factor and minimum gasket seating stress should be determined according to the design codes [13, 14] subject to gasket material and structural. These codes are based on a series of assumptions and might not define calculation procedures for sealing performance in detail [15]. Persson [16] and Kazeminia et al. [17] revaluated the leakage of metallic seal, which was used to design bolted flanged connections. Zhao et al. [18], established the mathematical relationship between the contact stress of metal sealing ring governing the sealing performance, the structural parameters and operating pressure, but did not consider the plastic deformation of metallic gasket. Sawa et al. [19] and Takaki et al. [20] studied the contact pressure on the sealing surface by elastic-plastic finite element analysis with regard of nonlinearity of gasket and internal pressure. However, the analysis is for the spiral wound gasket only. Nitta et al. [21], analyzed the critical contact pressure to eliminate the radial leakage paths by the quantitative analysis of the leakage, but did not discover the critical contact pressure to fully block the leakage paths. Using a finite element analysis approach, Joshi et al. [22], and Abid et al. [23] studied the flange connection without gasket, which concluded surface profiles, thickness of flange and bolt prestress had effects on the stress in the flange and bolts as well as flange rotation and displacement, but the effects on sealing performance wasn't investigated. Guindani et al. [24], studied the deformation recovery of sealing material and optimized the sealing performance of rubber. Bouzid et al. [25] and Wu et al. [26] proved the mean contact pressure and its distribution on sealing surface took important effects on sealing performance. By finite element analysis and experiment, Noga et al. [27] proved the suitable contact pressure and width of plastic deformation were the key parameters to guarantee the sealing performance of flange connection without gasket. However, the critical values of contact pressure and plastic deformation are not investigated. According to the above researches, the right contact pressure will make the plastic deformation happen on sealing surface and block micro leakage paths. Therefore, the contact pressure is essential for the optimal sealing performance of SPMC.

This paper aims to develop, demonstrate and validate an optimal design method of SPMC with the sealing performance. Based on the sealing structure of SPMC and static metal sealing mechanism, the critical condition of static metal seal is established for SPMC. On the base of superposition theorem of elasticity and compression experiment of the pipeline material, the minimum mean contact pressure of 8.625 inch SPMC is calculated. The parametric model of SPMC is created in APDL for optimization, with structure parameters of the sealing part as design variables, mean contact pressures and plastic strains on two sealing surfaces and variance of contact pressure on the second sealing surface as constrained variables, and minimum variance of contact pressure on the first sealing surface as objective function. The optimization is conducted by the zero-order method in ANSYS and water pressure experiments and bending experiments are carried out.

2 Structure and Installation of SPMC

2.1 Structure

SPMCs are used for non-weld connection of subsea oil-gas pipelines. Because of complicated subsea environment, SPMC should have a capacity to resist both of internal high pressure and external alternating load, such as axial tension and compression, bend and oscillation. The SPMC is composed of one basic body and two press rings, as shown in Figure 1. The basic body is axisymmetric about its central line, and its structure on both sides is symmetric about the mid-plane. The basic body consists of first sealing rings, first convex rings, second

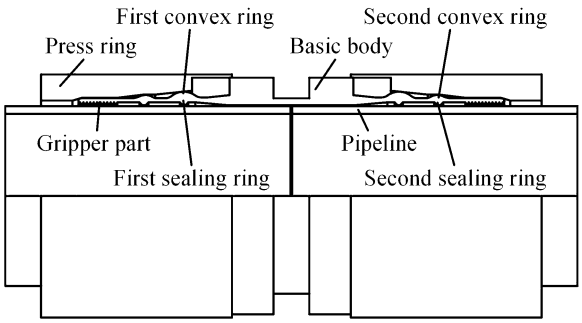

Figure 1 Structure schematic of SPMC

sealing rings, second convex rings and gripper parts from the central mid-plane to the far ends. Press rings are also axisymmetric about the central line, its external surface is cylindrical, and its internal surface is a profile that consists of cylindrical surfaces and conical surfaces. The press ring moves toward the middle of the basic body along the axial direction under clamping force produced by installation tool, and first sealing ring, second sealing ring and gripper part will shrink in the radial direction following the internal profile of the press ring. The axial displacement will make the two sealing rings touch the pipeline external surface and the sealing surfaces of the first and second sealing rings will be achieved, which prevents oil-gas from leaking. Meanwhile, the gripper parts will be embedded into the external surface of the pipeline and connect the pipelines as a whole piece, which will resist the external force and protect the sealing of SPMC from damage in submarine environment.

2.2 Installation

As a large amount of connections are required in oil-gas production system as well as pipelines repair, taking the advantage of the simple mechanical structure and short lead time, SPMCs can be used extensively. The connection process for the pipeline repair is shown in Figure 2. The first, the position of leakage is detected by inspection equipment; The second, the damaged section of the pipeline is cut by cutting tool and removed; The next, press rings and basic body are installed on the open ends of the pipeline, and the prefabricated pipe section is lowered down from the support vessel and located between the two SPMCs; In the end, SPMCs are pushed back to the butting points. The axial clamping forces push the press ring to the position limit, sealing surfaces are formed, and the repair is done.

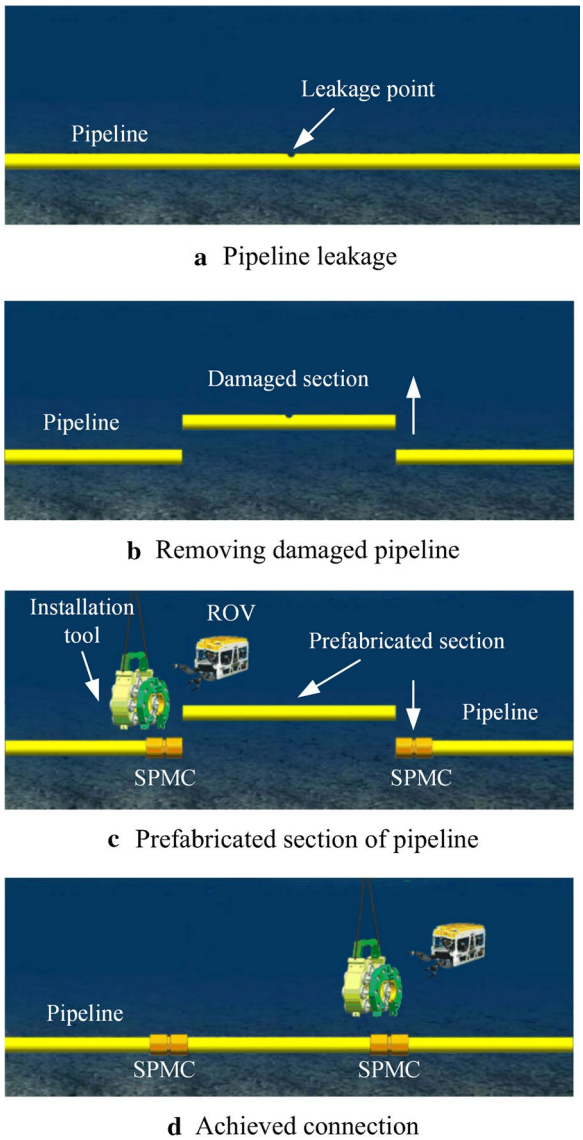

Figure 2 Connection process

3 Minimum Mean Contact Pressure

3.1 Sealing Mechanism

The static metal seal is adopted in SPMC. When two sealing rings shrink in the radial direction, two sealing surfaces will be created by the squeeze between internal surface of sealing ring and external surface of pipeline. As the sealing rings machined are not perfect and its roughness is a little better than that of pipeline, under the microscopy, the surfaces are overlaid by innumerable micro-peaks and micro-pits, which tend to form micro leakage paths, as shown in Figure 3. In order to realize an absolute static metal sealing, the squeeze quantity on sealing surfaces must reach a critical value, which creates enough contact pressure and makes elastic-plastic deformation happen within the metal seal as well as enough plastic flow to block micro leakage paths to achieve the static metal seal [28], as shown in Figure 4. The contact

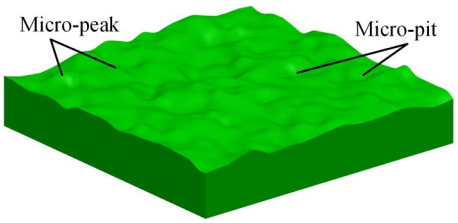

Figure 3 Micro surface

pressure and contact width on sealing surfaces are two important parameters for keeping seal work well [29, 30]. Bucher [31] and Wang et al. [32], concluded that the

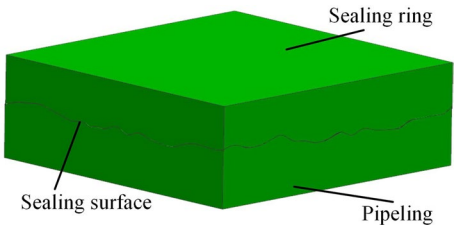

Figure 4 Sealing surface

contact width was no less than 1.6 mm and its contact pressure should be more than double of the yield strength of the pipeline material.

According to the characteristics of contact mechanics, the contact pressure is non-uniform, which is symmetric about the mid-plane of the sealing surface, as shown in Figure 5. When SPMCs achieve a reliable sealing, the critical condition of the contact pressure on sealing surface is

$$\begin{cases} P^{\mathrm{B}} = 2\sigma_{\mathrm{s}}, \\ P^{\mathrm{C}} = 2\sigma_{\mathrm{s}}, \\ L_{\mathrm{AB}} + L_{\mathrm{CD}} = 1.6\ \mathrm{mm}, \end{cases} \tag{1}$$

where P^{B} is the contact pressure at B, P^{C} is the contact pressure at C, σ_{s} is the yield strength of pipeline material, L_{AB} is the distance between A and B, and L_{CD} is the distance between C and D.

The minimum mean contact pressure, $\overline{P}_{\mathrm{AD}}$, is the mean contact pressure on sealing surface that meets Eq. (1), which represents the value and distribution of the contact pressure and can be used to evaluate sealing performance generally. In the optimization of SPMC, $\overline{P}_{\mathrm{AD}}$ is defined as a boundary condition for a reliable seal.

3.2 Elastic Mechanical Model

3.2.1 Approximate Solution

The assembly of SPMC and pipelines is 3D axisymmetric and in order to make solution more efficient the sealing can be idealized as a 2D problem. As the contact pressure is non-uniform, the model of approximate solution is shown in Figure 6. The distance between A and D, L_{AD}, is divided into n sections with equal width, and the width of each section is $l_i = L_{\mathrm{AD}}/n = l$. If n is big enough, we can assume the contact pressure p_i is uniform within a width of l_i. The equivalent mechanical model is n bands with uniform contact pressure p_i within each band applied on the external surface of the pipeline, where $i = 1, 2, \ldots, n$.

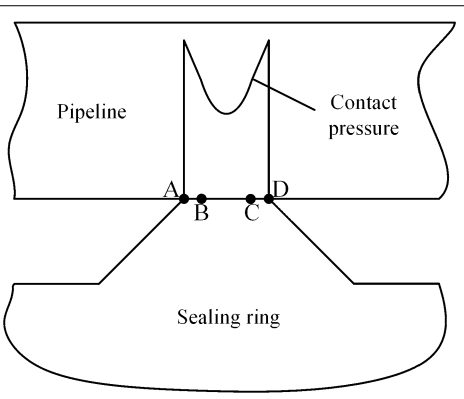

Figure 5 Contact pressure distribution

3.2.2 Single Pressure Band Solution

According to the superposition theorem, the mechanical model of pipeline under band l_1 of the pressure p_i is shown in Figure 7. The stress state in *orz* equals to the sum of the stress state in $o_1r_1z_1$ and that in $o_2r_2z_2$, and the equation is

$$\begin{cases} \sigma_m^1(r,z) = \sigma_m^{o_1}(r,z) + \sigma_m^{o_2}(r,z), \\ \sigma_m^{o_2}(r,z) = -\sigma_m^{o_1}(r,z-l), \end{cases} \tag{2}$$

where $\sigma_m^1(r,z)$ is the stress in *orz*, $\sigma_m^{o_1}(r,z)$ is the stress in $o_1r_1z_1$, and $\sigma_m^{o_2}(r,z)$ is the stress in $o_2r_2z_2$, $m = r, \theta, z, rz$.

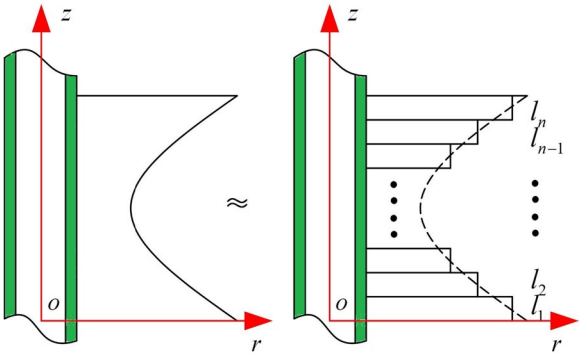

Figure 6 Approximate model of contact pressure

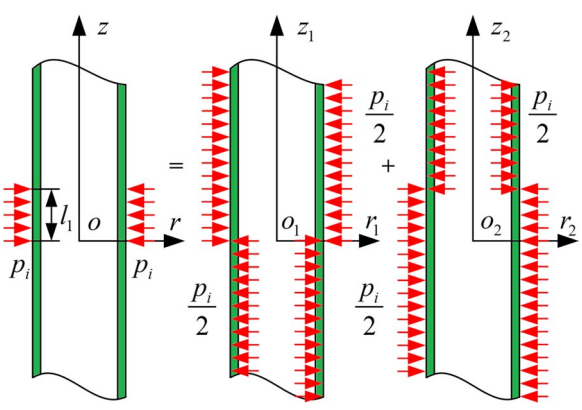

Figure 7 Mechanical model

The stress function method can be used to solve the stress of pipeline. Suppose the gravity is negligible, the relationships between stress components ($\sigma_r^{o_1}$, $\sigma_\theta^{o_1}$, $\sigma_z^{o_1}$, $\tau_{rz}^{o_1}$) and the stress function Ψ in $o_1r_1z_1$ are

$$\begin{cases} \sigma_r^{o_1} = \frac{\partial}{\partial z}\left(\mu\nabla^2\boldsymbol{\psi} - \frac{\partial^2\boldsymbol{\psi}}{\partial r^2}\right), \\ \sigma_\theta^{o_1} = \frac{\partial}{\partial z}\left(\mu\nabla^2\boldsymbol{\psi} - \frac{1}{r}\frac{\partial\boldsymbol{\psi}}{\partial r}\right), \\ \sigma_z^{o_1} = \frac{\partial}{\partial z}\left[(2-\mu)\nabla^2\boldsymbol{\psi} - \frac{\partial^2\boldsymbol{\psi}}{\partial z^2}\right], \\ \tau_{rz}^{o_1} = \tau_{zr}^{o_1} = \frac{\partial}{\partial r}\left[(1-\mu)\nabla^2\boldsymbol{\psi} - \frac{\partial^2\boldsymbol{\psi}}{\partial z^2}\right], \end{cases} \tag{3}$$

where μ is Poisson ratio, ∇^2 is Laplace operator, and its equation is

$$\nabla^2 = \frac{\partial^2}{\partial r^2} + \frac{1}{r}\frac{\partial}{\partial r} + \frac{\partial^2}{\partial z^2}. \tag{4}$$

Suppose the stress function is $\Psi = T(r)\cos(kz)$, taking it into Eq. (4), the result is

$$\frac{\partial^2 T(r)}{\partial r^2} + \frac{1}{r}\frac{\partial T(r)}{\partial r} - k^2 T(r) = 0. \tag{5}$$

Eq. (5) is correctional zero-order Bessel equation. Because the geometry model is a pipe, the general solution of Eq. (5) is

$$T(r) = a_0 I_0(kr) + a_1 kr I_1(kr) + b_0 K_0(kr) + b_1 kr K_1(kr), \tag{6}$$

where four coefficients, a_0, a_1, b_0 and b_1, are solved by boundary conditions of the mechanical model. $I_0(kr)$ and $I_1(kr)$ are the first kind correctional zero-order Bessel function and one-order Bessel function respectively. $K_0(kr)$ and $K_1(kr)$ are the second kind correctional zero-order Bessel function and one-order Bessel function respectively. kr is a public variable. The expressions are

$$\begin{cases} I_\nu(kr) = \sum\limits_{N=0}^{+\infty} \frac{1}{N!\tau(\nu+N+1)}\left(\frac{kr}{2}\right)^{\nu+2N}, \\ K_\nu(kr) = \lim\limits_{M\to\nu}\left\{\frac{\pi}{2\sin(M\pi)}[I_{-M}(kr) - I_M(kr)]\right\}, \end{cases} \tag{7}$$

where ν is equal to 0 or 1.

In Eq. (6), assuming $a_0 = e_1b_1$, $a_1 = e_2b_1$, $b_0 = e_3b_1$, $b_1 = b(k)\mathrm{d}k$, Ψ can be rewritten as

$$\begin{aligned} \boldsymbol{\Psi} = {} & \cos(kz)[e_1 I_0(kr) + e_2 kr I_1(kr) + e_3 K_0(kr) \\ & + krK_1(kr)]b(k)\mathrm{d}k. \end{aligned} \tag{8}$$

The general solution of Ψ is the integral of Eq. (8) with k from 0 to infinite:

$$\boldsymbol{\Psi} = \sum \boldsymbol{\Psi} = \int_0^{+\infty} b(k)\cos(kz)[e_1 I_0(kr) + e_2 kr I_1(kr) + e_3 K_0(kr) + krK_1(kr)]\mathrm{d}k. \tag{9}$$

In $o_1r_1z_1$, the boundary conditions of the pipeline are

$$\begin{cases} \sigma_r^{o_1}\big|_{r=r_{\text{in}}} = 0, \\ \sigma_r^{o_1}\big|_{r=r_{\text{out}}} = \frac{p_i}{\pi}\int_0^{+\infty}\frac{\sin(kz)}{k}\mathrm{d}k = \begin{cases} p_i/2, & z>0 \\ 0, & z=0 \\ -p_i/2, & z<0, \end{cases} \\ \tau_{rz}^{o_1}\big|_{r=r_{\text{out}},r_{\text{in}}} = 0, \end{cases} \tag{10}$$

where pipeline outer radius is r_{out} and its inner radius is r_{in}.

By solving Eqs. (3), (9), (10), the expressions (e_1, e_2, e_3, $b(k)$) are

$$\begin{pmatrix} e_1 \\ e_2 \\ e_3 \end{pmatrix} = \begin{pmatrix} G_1(kr_{\text{out}}) & G_2(kr_{\text{out}}) & G_3(kr_{\text{out}}) \\ G_1(kr_{\text{in}}) & G_2(kr_{\text{in}}) & G_3(kr_{\text{in}}) \\ H_1(kr_{\text{in}}) & H_2(kr_{\text{in}}) & H_3(kr_{\text{in}}) \end{pmatrix}^{-1} \begin{pmatrix} Q(kr_{\text{out}}) \\ Q(kr_{\text{in}}) \\ P(kr_{\text{in}}) \end{pmatrix}, \tag{11}$$

$$b(k) = \frac{p_i}{\pi k^4\begin{pmatrix} H_1(kr_{\text{out}}) & H_2(kr_{\text{out}}) & H_3(kr_{\text{out}}) \end{pmatrix}\begin{pmatrix} e_1 & e_2 & e_3 \end{pmatrix}^{\mathrm{T}} - P(kr_{\text{out}})}, \tag{12}$$

where

$$\begin{cases} G_1(kr) = I_1(kr), \\ G_2(kr) = krI_0(kr) + 2(1-\mu)I_1(kr), \\ G_3(kr) = -K_1(kr), \\ Q(kr) = krK_0(kr) - 2(1-\mu)K_1(kr), \\ H_1(kr) = I_0(kr) - I_1(kr)/(kr), \\ H_2(kr) = (1-2\mu)I_0(kr) + krI_1(kr), \\ H_3(kr) = K_0(kr) + K_1(kr)/(kr), \\ P(kr) = (1-2\mu)K_0(kr) - krK_1(kr). \end{cases} \tag{13}$$

Taking Eq. (12) into Eq. (9), the stress function, Ψ, can be rewritten as

$$\boldsymbol{\Psi} = p_i\int_0^{+\infty}\frac{\cos(kz)}{\pi k^4}\times\frac{\left[\begin{pmatrix} I_0(kr) & krI_1(kr) & K_0(kr) \end{pmatrix}\begin{pmatrix} e_1 & e_2 & e_3 \end{pmatrix}^{\mathrm{T}} + krK_1(kr)\right]}{\left[\begin{pmatrix} H_1(kr_{\text{out}}) & H_2(kr_{\text{out}}) & H_3(kr_{\text{out}}) \end{pmatrix}\begin{pmatrix} e_1 & e_2 & e_3 \end{pmatrix}^{\mathrm{T}} - P(kr_{\text{out}})\right]}\mathrm{d}k. \tag{14}$$

By solving Eqs. (2), (3) and (14), the stress state of a pipeline under band l_1 of the pressure p_i, $\sigma_r^1(r,z)$, $\sigma_\theta^1(r,z)$, $\sigma_z^1(r,z)$ can be expressed as

$$\begin{cases} \sigma_r^1(r,z) = p_i \int_0^{+\infty} \frac{1}{\pi} \frac{\sin(kz) - \sin[k(z-l)]}{k} \frac{\left[\left(H_1(kr)\ H_2(kr)\ H_3(kr) \right) \left(e_1\ e_2\ e_3 \right)^{\mathrm{T}} - P(kr) \right]}{\left[\left(H_1(kr_{\mathrm{out}})\ H_2(kr_{\mathrm{out}})\ H_3(kr_{\mathrm{out}}) \right) \left(e_1\ e_2\ e_3 \right)^{\mathrm{T}} - P(kr_{\mathrm{out}}) \right]} \mathrm{d}k, \\ \sigma_\theta^1(r,z) = p_i \int_0^{+\infty} \frac{1}{\pi} \frac{\sin(kz) - \sin[k(z-l)]}{k} \frac{\left(I_1(kr)/(kr)\ (1-2\mu) I_0(kr)\ -K_1(kr)/(kr) \right) \left(e_1\ e_2\ e_3 \right)^{\mathrm{T}}}{\left[\left(H_1(kr_{\mathrm{out}})\ H_2(kr_{\mathrm{out}})\ H_3(kr_{\mathrm{out}}) \right) \left(e_1\ e_2\ e_3 \right)^{\mathrm{T}} - P(kr_{\mathrm{out}}) \right]} \mathrm{d}k - \\ \qquad p_i \int_0^{+\infty} \frac{1}{\pi} \frac{\sin(kz) - \sin[k(z-l)]}{k} \frac{(1-2\mu) K_0(kr)}{\left[\left(H_1(kr_{\mathrm{out}})\ H_2(kr_{\mathrm{out}})\ H_3(kr_{\mathrm{out}}) \right) \left(e_1\ e_2\ e_3 \right)^{\mathrm{T}} - P(kr_{\mathrm{out}}) \right]} \mathrm{d}k, \\ \sigma_z^1(r,z) = p_i \int_0^{+\infty} \frac{1}{\pi} \frac{\sin(kz) - \sin[k(z-l)]}{k} \frac{\left(-I_0(kr)\ -2(2-\mu) I_0(kr) - kr I_1(kr)\ -K_0(kr) \right) \left(e_1\ e_2\ e_3 \right)^{\mathrm{T}}}{\left[\left(H_1(kr_{\mathrm{out}})\ H_2(kr_{\mathrm{out}})\ H_3(kr_{\mathrm{out}}) \right) \left(e_1\ e_2\ e_3 \right)^{\mathrm{T}} - P(kr_{\mathrm{out}}) \right]} \mathrm{d}k + \\ \qquad p_i \int_0^{+\infty} \frac{1}{\pi} \frac{\sin(kz) - \sin[k(z-l)]}{k} \frac{2(2-\mu) K_0(kr) - kr K_1(kr)}{\left[\left(H_1(kr_{\mathrm{out}})\ H_2(kr_{\mathrm{out}})\ H_3(kr_{\mathrm{out}}) \right) \left(e_1\ e_2\ e_3 \right)^{\mathrm{T}} - P(kr_{\mathrm{out}}) \right]} \mathrm{d}k. \end{cases} \tag{15}$$

According to elastic mechanics, physical equation and geometric equation of 3D axial symmetric model is

$$\begin{cases} \varepsilon_\theta^1 = \frac{1}{E}[\sigma_\theta^1 - \mu(\sigma_z^1 + \sigma_r^1)], \\ \varepsilon_\theta^1 = \frac{u_r^1}{r}. \end{cases} \tag{16}$$

Substitute Eq. (15) into Eq. (16), the radial displacement of the pipeline is

$$\begin{aligned} u_r^1(r,z) = p_i \int_0^{+\infty} \frac{(1+\mu)r}{E\pi} \frac{\sin(kz) - \sin[k(z-l)]}{k} \frac{\left(I_1(kr)/(kr)\ I_0(kr)\ -K_1(kr)/(kr) \right) \left(e_1\ e_2\ e_3 \right)^{\mathrm{T}}}{\left[\left(H_1(kr_{\mathrm{out}})\ H_2(kr_{\mathrm{out}})\ H_3(kr_{\mathrm{out}}) \right) \left(e_1\ e_2\ e_3 \right)^{\mathrm{T}} - P(kr_{\mathrm{out}}) \right]} \mathrm{d}k \\ - p_i \int_0^{+\infty} \frac{(1+\mu)r}{E\pi} \frac{\sin(kz) - \sin[k(z-l)]}{k} \frac{K_0(kr)}{\left[\left(H_1(kr_{\mathrm{out}})\ H_2(kr_{\mathrm{out}})\ H_3(kr_{\mathrm{out}}) \right) \left(e_1\ e_2\ e_3 \right)^{\mathrm{T}} - P(kr_{\mathrm{out}}) \right]} \mathrm{d}k. \end{aligned} \tag{17}$$

The radial displacement, u_r^i, of a pipeline under band l_i of the pressure p_i is equal to that of the pipeline under band l_1 of the pressure p_i which moves $(i-1)l$ along z axis direction. The radial displacement, u_r^i, is

$$\begin{aligned} u_r^i(r,z) = p_i \int_0^{+\infty} \frac{(1+\mu)r}{E\pi} \frac{\sin\{k[z-(i-1)l]\} - \sin[k(z-il)]}{k} \frac{\left(I_1(kr)/(kr)\ I_0(kr)\ -K_1(kr)/(kr) \right) \left(e_1\ e_2\ e_3 \right)^{\mathrm{T}}}{\left[\left(H_1(kr_{\mathrm{out}})\ H_2(kr_{\mathrm{out}})\ H_3(kr_{\mathrm{out}}) \right) \left(e_1\ e_2\ e_3 \right)^{\mathrm{T}} - P(kr_{\mathrm{out}}) \right]} \mathrm{d}k \\ - p_i \int_0^{+\infty} \frac{(1+\mu)r}{E\pi} \frac{\sin\{k[z-(i-1)l]\} - \sin[k(z-il)]}{k} \frac{K_0(kr)}{\left[\left(H_1(kr_{\mathrm{out}})\ H_2(kr_{\mathrm{out}})\ H_3(kr_{\mathrm{out}}) \right) \left(e_1\ e_2\ e_3 \right)^{\mathrm{T}} - P(kr_{\mathrm{out}}) \right]} \mathrm{d}k. \end{aligned} \tag{18}$$

3.2.3 Contact Pressure Solution

According to the analysis in Section 3.2.1, the radial displacement of any point in pipeline under n bands of contact pressure meets the superposition principle, and the total radial displacement is

$$u_r(r,z) = \sum_{i=1}^{n} u_r^i(r,z). \tag{19}$$

If n points are chosen with equal space along the pipeline, solving Eq. (19) inversely, the contact pressure, p_i, can be obtained

$$\begin{pmatrix} p_1 \\ p_2 \\ \vdots \\ p_n \end{pmatrix} = \begin{pmatrix} a_{11} & a_{12} & \cdots & a_{1n} \\ a_{21} & a_{22} & \cdots & a_{2n} \\ \vdots & \vdots & & \vdots \\ a_{n1} & a_{n2} & \cdots & a_{nn} \end{pmatrix}^{-1} \begin{pmatrix} u_r(r_1, z_1) \\ u_r(r_2, z_2) \\ \vdots \\ u_r(r_n, z_n) \end{pmatrix}, \tag{20}$$

where

$$a_{ji} = \int_0^{+\infty} \frac{(1+\mu)r_j}{E\pi} \frac{\sin\{k[z_j-(i-1)l]\} - \sin[k(z_j-il)]}{k} \frac{\begin{pmatrix} I_1(kr_j)/(kr_j) & I_0(kr_j) & -K_1(kr_j)/(kr_j) \end{pmatrix}\begin{pmatrix} e_1 & e_2 & e_3 \end{pmatrix}^{\mathrm{T}}}{\left[\begin{pmatrix} H_1(kr_{\mathrm{out}}) & H_2(kr_{\mathrm{out}}) & H_3(kr_{\mathrm{out}}) \end{pmatrix}\begin{pmatrix} e_1 & e_2 & e_3 \end{pmatrix}^{\mathrm{T}} - P(kr_{\mathrm{out}})\right]} \mathrm{d}k$$
$$- \int_0^{+\infty} \frac{(1+\mu)r_j}{E\pi} \frac{\sin\{k[z_j-(i-1)l]\} - \sin[k(z_j-il)]}{k} \frac{K_0(kr_j)}{\left[\begin{pmatrix} H_1(kr_{\mathrm{out}}) & H_2(kr_{\mathrm{out}}) & H_3(kr_{\mathrm{out}}) \end{pmatrix}\begin{pmatrix} e_1 & e_2 & e_3 \end{pmatrix}^{\mathrm{T}} - P(kr_{\mathrm{out}})\right]} \mathrm{d}k. \tag{21}$$

When $r_j = r_{\mathrm{out}}$, Eq. (20) will be the relationship between contact pressure and radical displacement of the pipeline external surface, and the expression is

$$\begin{pmatrix} p_1 \\ p_2 \\ \vdots \\ p_n \end{pmatrix} = \begin{pmatrix} a_{11}^* & a_{12}^* & \cdots & a_{1n}^* \\ a_{21}^* & a_{22}^* & \cdots & a_{2n}^* \\ \vdots & \vdots & & \vdots \\ a_{n1}^* & a_{n2}^* & \cdots & a_{nn}^* \end{pmatrix}^{-1} \begin{pmatrix} u_r^*(r_{\mathrm{out}}, z_1) \\ u_r^*(r_{\mathrm{out}}, z_2) \\ \vdots \\ u_r^*(r_{\mathrm{out}}, z_n) \end{pmatrix}. \tag{22}$$

3.3 Elastic-Plastic Solution

The sealing surface is formed by the squeeze between the internal surface of the sealing ring and the external surface of the pipeline, which makes the metal material on the sealing surface in a compression state and an elastic-plastic deformation occur. In the metal compression experiment of mild steel, the deformation of the metal is elastic firstly and then the metal starts to yield with further increase of compression, which is the elastic-plastic deformation. Eq. (22) is based on fully elastic deformation of metal material. However, when the stress σ_r on the sealing surface exceeds the yield stress of the metal material, plastic deformation will occur. With the same strain, the contact pressure obtained by Eq. (22) is bigger than that of elastic-plastic deformation.

Five test samples of the pipeline material had been prepared for compression experiments, which were carried out on universal material testing machine, WDW-3100. The result indicates that the mechanic property of pipeline material is composed of elastic and elastic-plastic parts clearly. Suppose the straight-line equation in elastic section and in elastic-plastic section is $y_{\mathrm{e}} = D_{\mathrm{e}}x$ and $y_{\mathrm{ep}} = D_{\mathrm{ep}}x + D_0$ respectively, using least square method, D_{e} can be regressed as 6722, D_{ep} as 2472, and D_0 as 162.9. The mean absolute error between theoretical results and test results is 8.48 MPa. The error bars is standard deviation and increases slightly with strain increasing, as shown in Figure 8. The error resources mainly include material property error, geometrical error, dimension error, load error and measuring error.

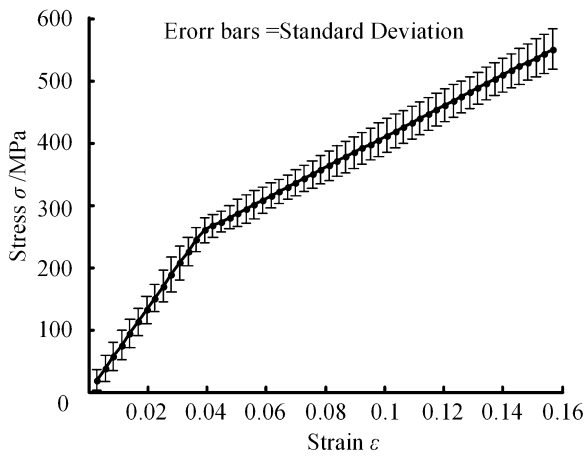

Figure 8 Compression experiment

With the same strain, elastic-plastic contact pressure p_i^* is

$$p_i^* = \begin{cases} \dfrac{D_{\mathrm{ep}}}{D_{\mathrm{e}}} p_i + D_0, & p_i > \sigma_{\mathrm{s}}, \\ p_i, & p_i \le \sigma_{\mathrm{s}}. \end{cases} \tag{23}$$

When elastic contact pressure on sealing surface, $\boldsymbol{P} = (p_1\ p_2\ \cdots\ p_n)^{\mathrm{T}}$, meets Eq. (1), $\bar{P}_{\mathrm{AD}}$ is the minimum mean contact pressure to realize a static metal seal for SPMCs, and the expression is

$$\bar{P}_{\mathrm{AD}} = \frac{1}{n} \sum_{i=1}^{n} p_i^*. \tag{24}$$

4 Optimization of 8 Inch SPMC

4.1 The Minimum Mean Contact Pressure

This paper takes 8.625 inch oil-gas pipelines in API 5L standards (Specification for line pipe) as an example to design SPMC. The outer radius of the pipeline, r_{out}, is 109.5 mm, its inner radius, r_{in}, is 100 mm, and its yield strength, σ_{s}, is 235 MPa. According to the design experience of static metal seal, the yield strength of SPMC is higher than that of pipeline, which makes plastic flow happen more on pipeline surface to achieve reliable

seal. Therefore, Q345 is selected for SPMC, and its yield strength is 345 MPa. There is also a minimum contact width for the sealing surface, otherwise leakage will happen. With regard of sealing reliability of SPMC, loading force for installation, and minimal effect on pipeline strength, the sealing width, L_{AD}, is 3 mm.

If $n = 10$, $l = L_{AD}/n = 0.3$ mm. $\boldsymbol{U} = (0.1999\ 0.2006\ 0.2012\ 0.2017\ 0.2019\ 0.2019\ 0.2017\ 0.2012\ 0.2006\ 0.1999)^{T}$ is taken into Eq. (22), and the contact pressure, p_i, can be obtained. Taking p_i into Eq. (23) and then Eq. (24), the minimum mean contact pressure, $\overline{P}_{AD}$, equals 361 MPa.

4.2 Analysis of Key Variables

The geometrical profile, constraints and boundary conditions are axisymmetric about the pipeline central line. In order to save computation time, the 2D model is used for the optimization of SPMCs. For a reliable seal, the mean contact pressure on the sealing surface should be higher than $\overline{P}_{AD}$, which equals 361 MPa. The variance of the contact pressure is defined as an uniformity coefficient of the contact pressure, which reflects whether the full contact on the sealing surface happens. By analyzing the structure of SPMC, five key structure dimensions have effects on the sealing performance.

L_1 is the distance between the mid-plane of the first sealing ring and the mid-plane of the first convex ring and affects the variance of the contact pressure on the first sealing surface; L_2 is the distance between the mid-plane of the second sealing ring and the mid-plane of the second convex ring and affects the variance of the contact pressure on the second sealing surface; H_1 is the shrinkage of the first sealing ring in the radial direction and affects the mean contact pressure on the first sealing surface; H_2 is the shrinkage of the second sealing ring in the radial direction and affects the mean contact pressure on the second sealing surface; L_3 is the relative distance between the first sealing ring and the second sealing ring and affects the interrelationship of them; as shown in Figure 9.

4.3 Finite Element Model

The parameterized model was created in APDL. Because the gripper part had no effect on sealing performance and its structure was too complicated to be meshed, the gripper teeth would be smoothed in finite element model, as shown in Figure 10. In order to improve the accuracy of the finite element analysis, the meshes on the first and the second sealing surfaces had be refined. There were four contact pairs in the finite element model. The first contact pair was between the first sealing ring and external surface of the pipeline, the second one was between the second sealing ring and external surface of the pipeline, the third one was between the first convex ring and internal surface of the press ring and the forth one was between the second convex ring and internal surface of the press ring. The boundary conditions included fixed constraint on the end of the pipeline and basic body,

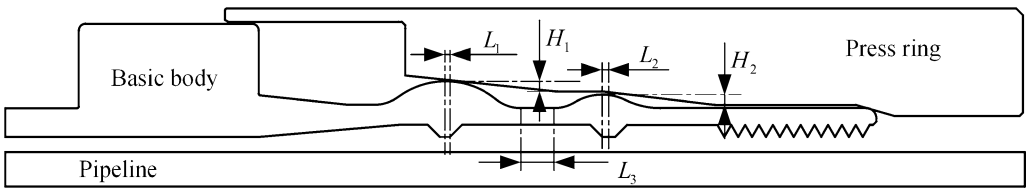

Figure 9 Key variables

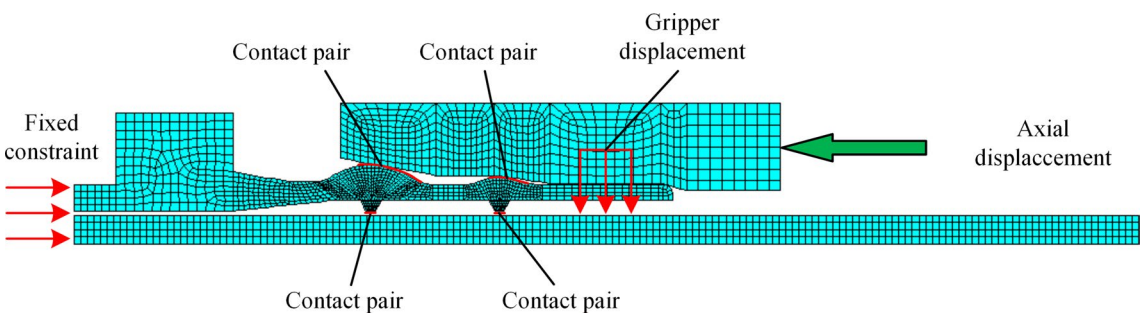

Figure 10 Finite element model

axial displacement at the end of the press ring, gripping displacement on the pipeline surface produced by the gripper.

(1) Constrained variables: $\overline{P}_{\text{first}}$ and $\overline{P}_{\text{second}}$ are the mean contact pressures on the first and the second sealing surface, which are the key factors to realize the sealing in SPMC, and their minimum value should be higher than 361 MPa. Because SPMCs are used in the complicated subsea environment, the sealing rings of SPMC should have a certain elasticity and stiffness, which will keep sufficient contact pressure on the sealing surface. Meanwhile, severe plastic deformation will reduce reliability of SPMC. The plastic strain of the first sealing surface, PS_{first}, and that of the second sealing surface, PS_{second}, should be as low as possible. The variance of contact pressure on second sealing surface, S^2_{second}, should be minimized to improve the sealing performance of SPMCs.

(2) Design variables: Five design variables are involved in this optimization, including L_1, L_2, H_1, H_2, and L_3, which are the key variables defined in Section 4.1, as shown in Figure 9.

(3) Objective function: Because the first sealing ring is the most important for SPMC, the mean contact pressure, $\overline{P}_{\text{first}}$, and the variance of the contact pressure, S^2_{first}, can be used to evaluate the sealing performance. When $\overline{P}_{\text{first}}$ is higher than 361 MPa, the lower S^2_{first}, represents the more uniform contact on the sealing surface and the higher the sealing reliability. Therefore, the minimum variance of contact pressure, S^2_{first}, can be defined as the objective function in this optimization.

Two optimization methods are available in ANSYS, which are the zero-order and one-order methods. Compared with zero-order method, one-order method has high calculation precision, but will cost a long computation time and tends to find a local optimal solution in design space. The zero-order method takes the advantages of short lead times, and its calculation precision meets the design requirement. The zero-order method has be used for optimization of SPMC, and the maximum number of iterations is 40.

4.4 Simulation Result

Figure 11(a) shows the variance of contact pressure S^2_{first} along with the number of iterations. S^2_{first} is fluctuant to decrease, and the optimal value is obtained in the 35th iteration. In the initial design, the variance of the contact pressure, S^2_{first}, equals to 26872.3, and decreases to 7413.6 after the optimization. Figure 11(b) shows the variance of

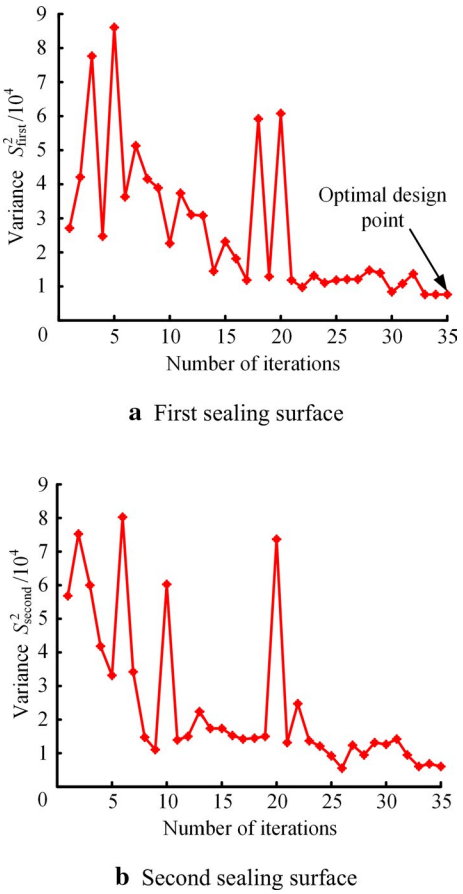

a First sealing surface

b Second sealing surface

Figure 11 Variance of contact pressure

second sealing surface, S^2_{second}, along with the number of iterations. In the initial design, the variance of the contact pressure, S^2_{second}, is 56623.4, and decreases to 6040.5 after the optimization. S^2_{first} and S^2_{second} decrease by 72.41% and 89.33% respectively. At the optimal point, because of the decrease of the variances of the contact pressure, the contact uniformity on two sealing surfaces will be improved significantly. For SPMCs, the improvement of uniformity will increase the effective contact width of the sealing surface, which will reduce the leakage possibility.

Figure 12 shows the mean contact pressures along with the number of iterations, which gradually increase. In the initial design of SPMCs, the mean contact pressures, $\overline{P}_{\text{first}}$, $\overline{P}_{\text{second}}$, are 305.41 MPa and 273.29 MPa respectively, and at the optimal point, they increase by 31.18% and 52.84% to 400.65 MPa and 417.69 MPa respectively, which are higher than 361 MPa and meets design requirement of the static metal seal. Figure 13 shows the plastic strains on first sealing surface and second sealing surface along with the number of iterations, which indicates that the values at the optimal point are less than 0.2, which will ensure a good elasticity and stiffness of the

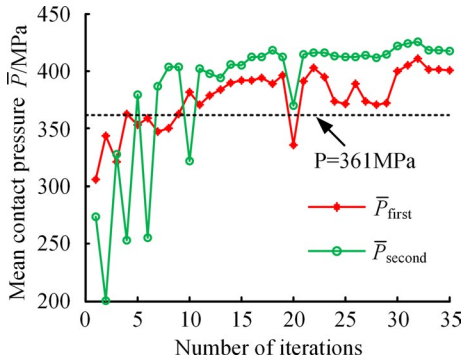

Figure 12 Contact pressure

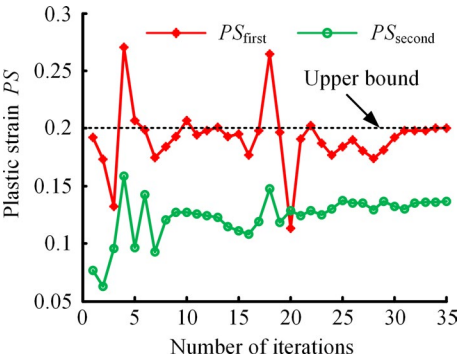

Figure 13 Plastic strain

sealing rings. The optimization improves adaptive ability of SPMCs in the complicated subsea environment.

The contact pressure distribution on the first sealing surface is shown in Figure 14. Before the optimization, the contact pressure distribution is non-uniform, and the contact pressure on the lower part of the first sealing surface is less than the yield strength, which will reduce the effective contact width. After the optimization, the mean contact pressure increases considerably, and the uniformity is improved. The effective contact width is equal to design width (L_{AD}=3 mm), which reduces the leaking possibility.

Figure 15 shows that the contact pressure distributions on the second sealing surface. Before the optimization, there is a gap on the upper part of the sealing surface, and the effective contact width is only half of design width,

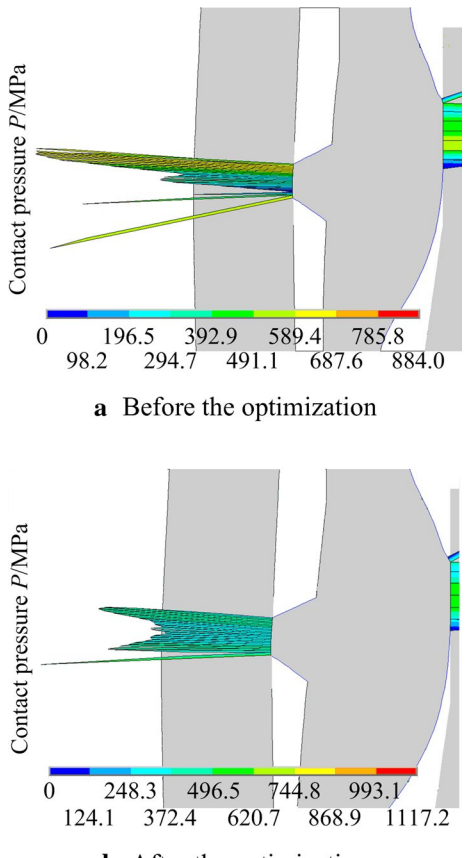

Figure 14 Contact pressure on first sealing surface

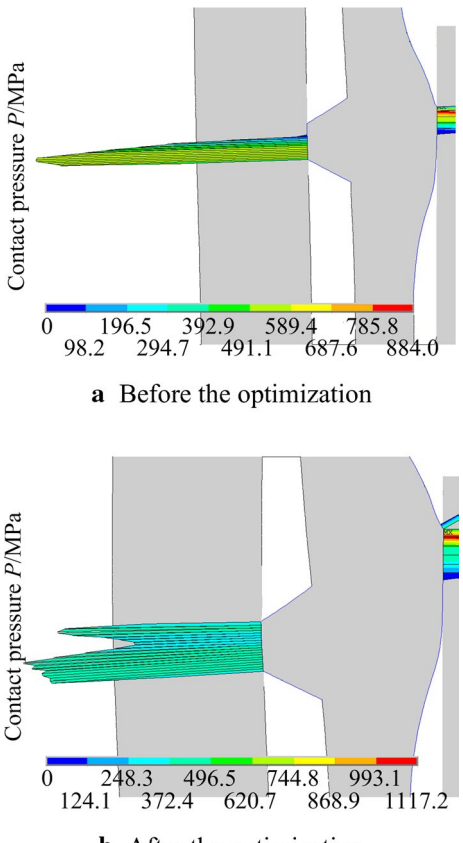

Figure 15 Contact pressure on second sealing surface

which trends to cause sealing failure under the complicated subsea environment. After the optimization, the mean contact pressure and uniformity are improved, and the internal surface of the sealing ring fully contacts the external surface of pipeline, which increases seal reliability.

5 Experiments

The rated pressure of SPMCs is 4.5 MPa. In order to verify the sealing performance of the optimized SPMCs, the water experiments and bending experiments are carried out according to the experiment codes for the mechanical connector [33]. Ten optimized SPMCs and ten non-optimized SPMCs are manufactured, ten SPMCs (five optimized SPMCs and five non-optimized SPMCs) are used for water pressure experiments, and the rest of SPMCs are used for bending experiments. The experimental system is composed of SPMCs, pipelines, pressure gage, shutoff valve, water hydraulic pump and electronic universal material testing machine (WEW3100). All experiments are carried out under the temperature of 20 °C.

5.1 Water Pressure Experiment

The schematic diagram of the water pressure experiment is shown in Figure 16. The experimental procedure is: the first, assembling experimental platform; the second, emptying gases in SPMCs, increasing an internal pressure of 2 MPa in every five minutes by the water hydraulic pump and turning off the shutoff valve; in the end, in pressure maintaining, the change of the pressure gauge is recorded, as well as the water leakage and relative displacement between pipelines and SPMC. When the internal pressure is increased, if the value of pressure gauge starts to drop, or leakage occurs, the value of the pressure gauge will be the maximum water pressure for the given SPMC. Figure 17 shows experimental facility of the water pressure experiment.

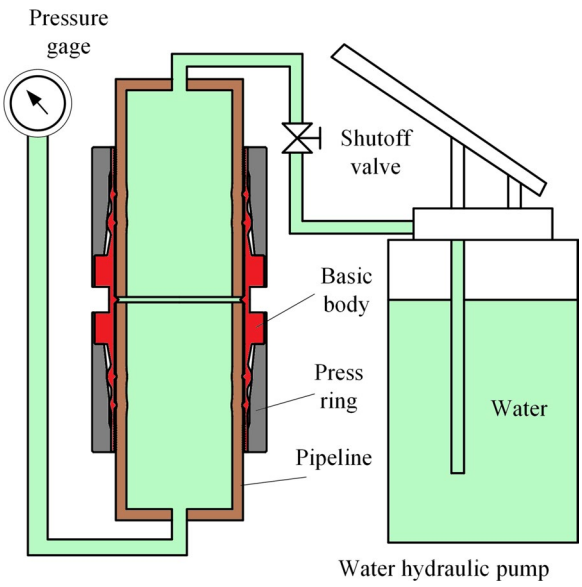

Figure 16 Schematic diagram

Table 1 shows the results of the water pressure experiments for SPMCs, which indicate there are no leakage and relative displacement for the ten SPMCs. The maximum pressure of all the optimized SPMCs is higher than the rated pressure of 4.5 MPa, and two of them have a pressure drop with the maximum pressures 48 MPa and 46 MPa, respectively. Only 40% of the non-optimized SPMCs meet design requirements. A big variation can be seen in the maximum pressure of the five non-optimized SPMCs, The variation of the pipeline parameters affects the mean contact pressure and variance on the sealing surface, which prevents a full contact between the sealing

Figure 17 Experimental facility

Table 1 Result of water pressure experiment

Class	Group	Experimental results			
		Pressure/MPa	Status	Leakage	Displacement
Optimized	First	48	Drop	No	No
	Second	50	No change	No	No
	Third	50	No change	No	No
	Fourth	46	Drop	No	No
	Fifth	50	No change	No	No
Non-optimized	First	4	Drop	No	No
	Second	2	Drop	No	No
	Third	4	Drop	No	No
	Fourth	14	Drop	No	No
	Fifth	8	Drop	No	No

rings and pipeline. The failure of the first sealing surface produces a pressure drop, and water get into the chamber between the first sealing surface and the second sealing surface. As the leakage is blocked by the second sealing surface, no water outflow can be seen. No relative displacements happen between SPMC and pipeline, which indicates the gripper produced pipe holding is strong enough. The water pressure experiments show that the optimization will improve the sealing performance of SPMCs considerably.

5.2 Bending Experiment

The schematic diagram of the bending experiment is shown in Figure 18. The length of the assembled SPMC, L_g, is 522 mm, and the parameter, L_p, is 500 mm according to the experiment codes. The experimental procedure is as follows: the first, assemble the experimental platform; the second, emptying gases in SPMCs, increasing water pressure in SPMC to the rated pressure of 4.5 MPa and turning off the shutoff valve; the next, the force, F, will be increased by 10 kN in every five minutes; in the end, in pressure maintaining, the change of the pressure gauge is recorded, as well as the water leakage. When the force is increased, if the value of pressure gauge starts to drop, or leakage occurs, the bending moment is the maximum bending moment of the given SPMC. Figure 19 shows the experimental facility of the bending experiment.

Table 2 lists the results of the bending experiments for the ten SPMCs, which indicate there are no leakages for both of the optimized and non-optimized SPMCs. Under bending moment of 52.2 kN·m (WEW3100 maximum capability), the pressure drops of the five optimized SPMCs are 0 MPa. One in five (20%) of the non-optimized SPMCs can bear the bending moment of 52.2 kN·m without pressure drop and leakage. The sealing of the third and fourth non-optimized SPMC failed without bending moment under the rated pressure of 4.5 MPa. The experimental results show that the optimization increases the bending resistance of SPMCs significantly.

By the contrast water pressure experiments and bending experiments for optimized and non-optimized

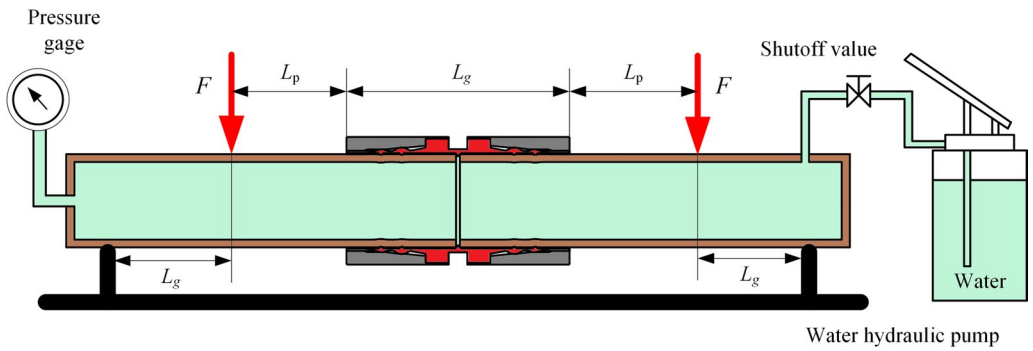

Figure 18 Schematic diagram

Figure 19 Experimental facility

Table 2 Result of bending experiment

Class	Group	Experimental results			
		F/kN	*M*/(kN·m)	Pressure	Leakage
Optimized	First	100	52.2	No change	No
	Second	100	52.2	No change	No
	Third	100	52.2	No change	No
	Fourth	100	52.2	No change	No
	Fifth	100	52.2	No change	No
Non-optimized	First	30	15.66	Drop	No
	Second	100	52.2	No change	No
	Third	0	0	Drop	No
	Fourth	0	0	Drop	No
	Fifth	50	26.1	Drop	No

SPMCs, the sealing ability of all optimized SPMCs is higher than rated pressure of 4.5 MPa, and no pressure drop can be seen under the bending moment of 52.2 kN·m.

6 Conclusions

(1) A cost efficient and practical connector is proposed on the base of static metal sealing mechanism. The critical condition of the contact pressure realizing a reliable static metal sealing on sealing surface is established.

(2) The minimum mean contact pressure of the sealing surface is formulated to support SPMC optimization and design. The minimum mean contact pressure of the 8.625 inch connector is calculated as 361 MPa.

(3) After the optimization of the sealing performance of SPMC, the variances of contact pressure on two sealing surfaces, S^2_{first}, S^2_{second}, decrease by 72.41% and 89.33%, respectively; the mean contact pressures on two sealing surfaces, $\overline{P}_{\text{first}}$, $\overline{P}_{\text{second}}$, increase by 31.18% and 52.84%, respectively. The decrease of variance makes the contact of sealing surface more uniform and the increase of the contact pressure makes the contact of sealing surface continuous, which improves the sealing performance considerably.

(4) The results indicate that in the water pressure experiments, the maximum pressure of 5 optimized SPMCs is much higher than the rated pressure of 4.5 MPa, but only 2 in 5 (40%) of the non-optimized SPMCs meet requirements; under bending moment of 52.2 kN·m, the pressure of the 5 optimized SPMCs does not change, but 1 in 5 (20%) of the non-optimized SPMCs have no pressure drop under maximum bending moment. The ability of the optimized SPMCs is much better than that of the non-optimized ones in both of the water pressure experiment and bending experiment.

Authors' contributions

LW leaded all team works and participated in the entire process, guided derivation of the optimal design method. ZW carried out the critical condition of the sealing performance for the connector and the formulation method of the contact pressure on the sealing surface. SY reviewed and contributed to this article with important proposals in both theoretical study and experimental study. YG and SL, both showed excellent skills in experimental study with many constructive comments. All authors read and approved the final manuscript.

Author details

[1] College of Mechanical and Electrical Engineering, Harbin Engineering University, Harbin 150001, China. [2] Advanced Manufacturing Research Centre with Boeing, The University of Sheffield, Sheffield S605TZ, UK.

Authors' Information

Li-Quan Wang born in 1957, is presently a professor at *College of Mechanical and Electrical Engineering, Harbin Engineering University, China*. He has been a Principal Investigator of a large variety of funded research work regarding the underwater equipment design and robot technology. His activities are documented by an extensive publication record of scientific papers, books and technical reports. He received various national awards for his overall research work and his scientific contributions to ocean engineering.

Zong-Liang Wei born in 1985, is currently a PhD candidate at *College of Mechanical and Electrical Engineering, Harbin Engineering University, China*. He has been an investigator in a national research project of the research of sealing principle and multi-objective optimization about a new type subsea pipeline compression mechanical connector funded by National Natural Science Foundation of China (No. 51279042) and Study on sealing mechanism of large diameter lens gasket based on deepwater pipeline connection funded by National Natural Science Foundation of China (No. 51105088). He research interests include static metal sealing mechanism, multi-objective optimization and reliability of pipeline connector.

Shao-Ming Yao born in 1967, is presently a professor at *Advanced Manufacturing Research Centre with Boeing, The University of Sheffield, UK*. His research interests include mechanical structure design, numerical simulation technology and lubrication technology. His activities are documented by publications in scientific papers.

Yu Guan born in 1990, is a master degree candidate at *College of Mechanical and Electrical Engineering, Harbin Engineering University, China*. His research interests are mechanical design and reliability design.

Shao-Kai Li born in 1990, is currently a master candidate at *College of Mechanical and Electrical Engineering, Harbin Engineering University, China*. His research interests are mechanical design and Rubber sealing technology.

Acknowledgements

Supported by National Natural Science Foundation of China (Grant Nos. 51279042, 51105088).

Competing interests

The authors declare that they have no competing interests.

Ethics approval and consent to participate

Not applicable.

Publisher's Note

Received: 22 January 2016 Accepted: 14 January 2018
Published online: 27 February 2018

References

[1] L Q Wang, C D Wang, J Liu. Error analysis and prototype testing of deepwater pipe flange connection tool. *Proceedings of the Institution of Mechanical Engineers Part C-Journal of Mechanical Engineering Science,* 2013, 288(11): 1978–1993.

[2] W M Wang, L Q Wang, C D Wang. A novel deepwater structure pose measurement method and experimental study. *Measurement*, 2012, 45(5): 1151–1158.

[3] L Q Wang, H Y Gong, X D Xing, et al. Rigid dynamic performance simulation of an offshore pipeline plough. *Ocean Engineering*, 2015, 94: 51–66.

[4] A Jasper. Oil/Gas pipeline leak inspection and repair in underwater poor visibility conditions: challenge and perspective. *Journal of Environmental Protection*, 2012, 3(5): 394–399.

[5] B E Morris. *Tapping connector and method of using same*: USA, US6691733B1. 2004–2–17.

[6] J W Pallini JR, S Wrong. *External hydraulic tieback connector*: USA, US9062513B2. 2015–6–23.

[7] K V Trepka, S Caspersen. *Subsea tool for tie in of pipeline ends*: USA, US6997645B2. 2006–2–14.

[8] D L Ford. *Adapter sleeve for wellhead housing*: USA, US7798231B2. 2010–9–21.

[9] B H Van Bilderbeek. *Pipeline joint*: USA, US7344162B2. 2008–3–18.

[10] J Hartmann, A Kaufmann, S Gelbrich, et al. *Coupling device*: USA, US20140008911A1. 2014–1–9.
[11] H Gottfried. *Coupling device for establishing a permanent non-removable pipe connection*: World Intellectual Property Organization, WO, 2005/068888A1. 2005–7–28.
[12] C Marie, D Lasseux. Experiment leak-rate measurement through a static metal seal. *Journal of Fluids Engineering*, 2007, 129(6): 799–805.
[13] American Society of Mechanical Engineers. *ASME BPVC-VIII-I Rules for construction of pressure vessels*. New York: American Society of Mechanical Engineers, 2007.
[14] Deutsches Institute für Normung. *DIN 2696 1999-08 Lenticular Ring Joint Gaskets for Flanged Joints*. Berlin: Deutsches Institute für Normung, 1999.
[15] M M Krishna, M S Shunmugam, N S Prasad. A study on the sealing performance of bolted flange joints with gaskets using finite element analysis. *International Journal of Pressure Vessels and Piping*, 2007, 84(6): 405–411.
[16] B N J Persson. Leakage of metallic seals: role of plastic deformations. *Tribology Letters*, 2016, 63(3): 1–6.
[17] M Kazeminia, A H Bouzid. Evaluation of leakage through graphite-based compression packing rings. *Journal of Pressure Vessel Technology*, 2016, 139(1): 011602(1–7).
[18] H L Zhao, R Chen, X L Luo, et al. Metal sealing performance of subsea X-tree wellhead connector sealer. *Chinese Journal of Mechanical Engineering*, 2015, 28(3): 649–656.
[19] T Sawa, N Ogata. Stress analysis and the sealing performance evaluation of pipe flange connection with spiral wound gaskets under internal pressure. *ASME Pressure Vessels and Piping Conference*, Vancouver, Canada, August 5–9, 2002: 115–127.
[20] T Takaki, T Fukuoka. Three-dimensional finite element analysis of pipe flange connections: the case of using compressed asbestos sheet gasket. *ASME Pressure Vessels and Piping Conference*, Vancouver, Canada, August 5–9, 2002: 171–177.
[21] I Nitta, Y Matsuzaki, Y Tsukiyama, et al. Thorough observation of real contact area of copper gaskets using a laser microscope with a wide field of view. *Journal of Tribology*, 2013, 135(4): 041103(1–7).
[22] D Joshi, P Mahadevan, A Marathe, et al. Unimportance of geometric nonlinearity in analysis of flanged joints with metal-to-metal contact. *International Journal of Pressure Vessels and Piping*, 2007, 84(7): 405–411.
[23] M Abid, D H Nash. A parametric study of metal-to-metal contact flanges with optimized geometry for safe stress and no-leak conditions. *International Journal of Pressure Vessels and Piping*, 2004, 81(1): 67–74.
[24] M Guindani, G Ramorino, S Agnelli, et al. Optimization of the sealing performance in transient conditions of rubber based hybrid nanocomposites by carbon nanotubes, as assessed by a tailored recovery test. *Polymer Testing*, 2016, 56: 229–236.
[25] A Bouzid, A Chaaban, A Bazergui. The influence of the flange rotation on the leakage performance of bolted flanged joints. *Proceedings of the CSME Forum*, Montreal, Canada, June 27–29, 1994: 184–194.
[26] D Wu, S P Wang, X J Wang. A novel stress distribution analytical model of O-ring seals under different properties of materials. *Journal of Mechanical Science and Technology*, 2017, 31(1): 289–296.
[27] N A Noga, M Nagawa, F Shiraishi, et al. Sealing performance of new gasketless flange. *Journal of Pressure Vessels Technology*, 2002, 124(2): 239–246.
[28] F Robbe-valloire, M Prat. A model for face-turned surface microgeometry application to the analysis of metallic static seals. *Wear*, 2008, 264(11–12): 980–989.
[29] A H Bouzid, M Dlany, M Derenne. Determination of gasket effective width based on leakage. *ASME/JSME 2004 Pressure Vessels and Piping Conference*, California, America, July 25–29, 2004: 105–111.
[30] M A Choiron, Y Kurata, S Haruyama, et al. Simulation and experimentation on the contact width of new metal gasket for asbestos substitution. *International Journal of Aerospace and Mechanical Engineering*, 2011, 75: 283–287.
[31] H H Bucher. *Industrial sealing technology*. Beijing: Chemical Industry Press, 1988. (in Chinese).
[32] L Q Wang, Z L Wei, Y Guan, et al. A novel subsea pipeline connection method and experimental study. *Proceedings of the 26th International Ocean and Polar Engineering Conference,* Rhodes, Greece, June 26–July 2, 2016: 907–913.
[33] International Organization for Standardization. *ISO 21329 Petroleum and Natural Gas Industries-Pipeline Transportation Systems-Test Procedures for Mechanical Connectors*. Switzerland: International Organization for Standardization, 2004.